

Elastic Scattering of 0.8-GeV Protons from ^{12}C , ^{58}Ni , and ^{208}Pb

G. S. Blanpied, W. R. Coker, R. P. Liljestrand, and L. Ray
University of Texas, Austin, Texas 78712

and

G. W. Hoffman
University of Texas, Austin, Texas 78712, and Los Alamos Scientific Laboratory, Los Alamos, New Mexico 87545

and

D. Madland, C. L. Morris, J. C. Pratt, J. E. Spencer, and H. A. Thiessen
Los Alamos Scientific Laboratory, Los Alamos, New Mexico 87545

and

N. M. Hintz, G. S. Kyle, and M. A. Oothoudt
University of Minnesota, Minneapolis, Minnesota 55455

and

T. S. Bauer, J. C. Fong, G. Igo, R. J. Ridge, and C. A. Whitten, Jr.
University of California, Los Angeles, California 90024

and

T. Kozlowski
Brookhaven National Laboratory, Upton, New York 11973

and

D. K. McDaniels and P. Varghese
University of Oregon, Eugene, Oregon 97403

and

P. M. Lang, H. Nann, and K. K. Seth
Northwestern University, Evanston, Illinois 60201

and

C. Glashausser
Rutgers University, New Brunswick, New Jersey 08903
(Received 1 September 1977)

Differential cross sections for elastic scattering of 0.8-GeV protons from ^{12}C , ^{58}Ni , and ^{208}Pb have been measured. Preliminary analysis of the data in terms of the Kerman-McManus-Thaler formalism with spin-dependent nucleon-nucleon amplitudes shows sensitivity to details of proton and neutron matter distributions.

Although recent electron scattering studies show considerable sensitivity to details of nuclear charge distributions,^{1,2} these studies have the essential limitation that they probe only the electromagnetic form factors of the nucleus,³ i. e., the charge distribution, and the magnetic moment distribution of an unpaired nucleon. Recent measurements of proton-nucleus elastic scattering at incident proton energies near 1 GeV have reawakened interest in what can be learned con-

cerning the nuclear matter distribution from hadron scattering. There are many recent theoretical papers on this subject.⁴⁻⁷ When such data extend to high enough momentum transfer [> 0.3 (GeV/c)²], the angular distributions display considerable sensitivity to rather fine details of the proton and neutron distributions, including density fluctuations in the nuclear interior, as we show here.

In this Letter, we report the first angular dis-

tributions for elastic scattering of 0.8-GeV protons from ^{12}C , ^{58}Ni , and ^{208}Pb obtained using the high-resolution spectrometer (HRS) at the Clinton P. Anderson Meson Physics Facility (LAMPF) of the Los Alamos Scientific Laboratory, along with a preliminary theoretical analysis.

The experimental system consists of a beam line dispersion matched to a quadrupole-dipole-dipole spectrometer which operates in the "momentum-loss" mode. The scattering and dispersion planes are orthogonal, such that focal-plane position perpendicular to the dispersion axis is proportional to scattering angle in the reaction plane. Focal-plane-position information was provided by two $60\text{ cm} \times 10\text{ cm}$ two-dimensional delay-line chambers, separated by 0.5 m. Four scintillators spaced over a 2-m interval provided pulse-height and time-of-flight information for particle identification. A fourfold coincidence among these scintillators provided the event trigger for the PDP11/45 computer in which the data were accumulated. Relative beam current monitoring was done with two ionization chambers placed 1 m behind the target in the 2-m-diam scattering chamber, a split secondary-emission monitor 3 m downstream from the target, and two four-counter particle telescope arrays which were located in the scattering plane at 45° and 135° relative to the target. The energy resolution obtained during the experiment ranged from 100 keV for the forward-angle measurements on ^{58}Ni and ^{208}Pb to about 350 keV for the backward-angle measurements on ^{12}C . As the HRS has an angular acceptance of about 3° in the plane of scattering, the spectrometer was moved in 1.5° – 2.0° increments in order to obtain good data overlap. Angle bins were chosen so that successive data points were separated by about 0.2° , which is also on the order of the overall instrumental angular resolution. Overall normalization of the data was obtained by taking (p,p) data on a CH target and normalizing to the $\text{H}(p,p)$ data of Willard *et al.*⁸ These normalization measurements were made during each running period when proton-nucleus data were accumulated. The absolute normalization of the data is believed reliable to within $\pm 15\%$ in overall magnitude.

The experimental data are shown in Fig. 1 together with results of a preliminary analysis. The analysis was carried out in the partial-wave

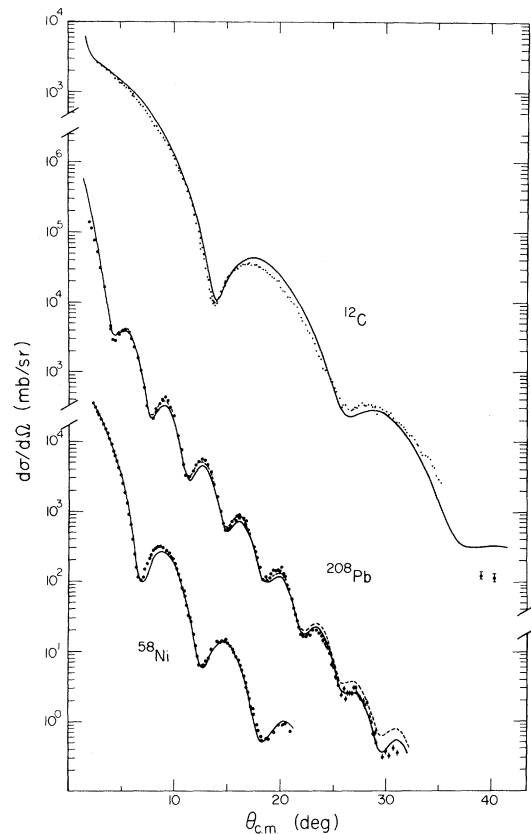


FIG. 1. Differential cross sections for 800-MeV proton elastic scattering from ^{12}C , ^{58}Ni , and ^{208}Pb . Error bars shown are statistical only, and where no error bars are present, the statistical errors are smaller than the size of the data points. The solid and dashed curves are discussed in the text.

formalism, solving the Schrödinger equation with exact relativistic kinematics.⁹ The proton-nucleus optical potential was obtained from the Kerman-McManus-Thaler expansion in the rearrangement discussed by Feshbach *et al.*¹⁰ In this approach, to first order in intermediate excitations of the target nucleus, the proton-nucleus optical potential is given in terms of the proton-nucleon scattering amplitudes and the matter density distributions of the target nucleus.¹⁰ We have adopted a general spin-dependent form for the nucleon-nucleon amplitudes:

$$t_{pj}(q^2) = t_{pj}^0(q^2) + it_{pj}^s(q^2)(\vec{\sigma}_p + \vec{\sigma}_j) \cdot \hat{n}, \quad (1)$$

where j stands for p or n , $\vec{q} = \vec{k}_i - \vec{k}_f$, and $\hat{n} = (\vec{k}_i \times \vec{k}_f) / |\vec{k}_i \times \vec{k}_f|$. The parametrization adopted is,¹¹ with M the nucleon mass,

$$\begin{aligned} t_{pj}^0(q^2) &= (ik_0 \sigma_{pj}^T / 4\pi)(1 - i\alpha_{pj}) \exp(-B_{pj}q^2), \\ t_{pj}^s(q^2) &= (ik_0 \theta_{pj} / 4\pi)(q^2 / 4M^2)^{1/2} (1 - i\alpha_{s,pj}) \exp(-B_{s,pj}q^2). \end{aligned} \quad (2)$$

TABLE I. The first six columns give the point-nucleon density parameters of Eq. (3) of the text used to generate the curves shown in Fig. 1. The quantity $\langle r^2 \rangle^{1/2}$ refers to the root-mean-square (rms) radius of the distribution. Variations of ± 0.03 fm in the rms radii produced no deterioration in any of the fits. The last three columns give the values of the spin-dependent parameters of Eq. (2) which give fair fits to preliminary proton-nucleus analyzing-power data.

Nucleus	w	R (fm)	z (fm)	s	r_0 (fm)	d (fm ⁻²)	$\langle r^2 \rangle^{1/2}$ (fm)	$\bar{\theta}_p$ (fm ²)	$\bar{\alpha}_{sp}$	$\bar{B}_{s,p}$ (fm ²)	
¹² C	p	-0.152	2.418	0.449	0.267	1.427	6.870	2.319	15.0	0.31	0.05
	n	-0.010	2.270	0.428	0.250	0.500	0.500	2.325	15.0	0.31	0.05
⁵⁸ Ni	p	-0.130	4.298	0.472	3.688	14.6	0.46	0.10
	n	-0.111	3.972	0.589	3.677	14.6	0.46	0.10
²⁰⁸ Pb ^a	p	0.130	6.590	0.475	5.460	11.0	0.58	0.09
	n	0.130	6.450	0.725	5.760	11.0	0.58	0.09
²⁰⁸ Pb ^b	p	0.130	6.590	0.475	0.440	3.300	1.360	5.360	11.0	0.58	0.09
	n	0.130	6.450	0.725	0.440	3.300	1.360	5.650	11.0	0.58	0.09

^aDashed curve, Fig. 1.

^bSolid curve, Fig. 1.

In principle, the twelve parameters of Eq. (2) may be determined by fitting proton-nucleon angular distributions and polarizations at a laboratory energy of 800 MeV. Keeping the empirical total cross sections σ_{pp}^T and σ_{pn}^T fixed at 4.73 and 3.80 fm², respectively, we fit the proton-nucleon data of Bystricki *et al.*¹² using Eq. (2) to obtain $\alpha_{pp} = 0.056$, $\alpha_{pn} = -0.20$ and $B_{pp} = 0.09$ fm², $B_{pn} = 0.12$ fm². With no data available as yet on nucleon-nucleon polarization at 800 MeV, we elected for the present to estimate values of θ_{pj} , $\alpha_{s,pj}$, and $B_{s,pj}$ from a first-order empirical fit to preliminary proton-nucleus polarization data at 800 MeV.¹³ Since little or nothing is known *a priori* concerning these six parameters, we had little choice but to reduce them to three

by finding instead the corresponding isospin-averaged parameters $\bar{\theta}_p$, $\bar{\alpha}_{s,p}$ and $\bar{B}_{s,p}$. These three parameters can be determined relatively unambiguously by fitting the nucleon-nucleon scattering, proton-nucleus scattering, and proton-nucleus polarization data simultaneously. Because our three target nuclei do not have the same N/Z ratio, we of course get different isospin-averaged parameters for the three different nuclei considered. The three parameters are given in Table I.

For the purposes of the present calculations, a general form for the point-nucleon matter density was adopted, consisting of a three-parameter Fermi distribution with a Gaussian correction term²:

$$\rho_j(r) = \rho_{0j} \left\{ (1 + w_j r^2 / R_j^2) [1 + \exp((r - R_j)/z_j)]^{-1} + s_j \exp(-d_j(r - r_{0j})^2) \right\}, \quad (3)$$

for $j = p$ or n .

In order to obtain the proton matter density parameters, the proton charge density was numerically unfolded from the nuclear density as determined by electron scattering.¹⁻³ As usual, ρ_{0j} was obtained by normalizing to the proper number of target nucleons.

For the case of ¹²C, unfolding the charge density given by Sick and McCarthy,² which is already in the form of Eq. (3), gave the point-proton matter density parameters shown in Table I. We then freely adjusted the corresponding parameters of the neutron density distribution to obtain the fit shown in Fig. 1 by the solid curve. We find that any neutron distribution with $\langle r^2 \rangle_n^{1/2}$

$= 2.325 \pm 0.030$ fm gives a good fit to the data up to the second maximum (18°). For the particular fit shown, the neutron density parameters are presented in Table I. The extracted difference between the neutron and proton rms radii, Δr_{np} , is consistent with zero, as expected. An inspection of the point-nucleon density parameters in Table I indicates considerable differences between the shapes of the two distributions. This difference is somewhat misleading, since the nucleon density distributions, obtained by folding the finite nucleon size into the point-nucleon densities of Table I, are, in fact, remarkably similar except in the region within 1 fm of the

origin. However, if the *same* parameters are used for both proton and neutron point-nucleon distributions, a poor fit is obtained beyond 25° . Thus rather slight differences in the shape of the matter densities are detectable.

For ^{58}Ni , the proton parameters (see Table I) were obtained by unfolding the three-parameter Fermi charge distribution of Ref. 3. The fit shown in Fig. 1 was obtained using the neutron parameters given in Table I. Again, we find $\Delta r_{np} \approx 0$, as expected.

Finally, we show for the ^{208}Pb data a further illustration of the sensitivity of the calculations to the interior behavior of the nuclear matter densities. The dashed curve is the result of a calculation with a three-parameter Fermi form, in which the proton parameters are again obtained (see Table I) by unfolding the charge density,^{4,3} and corresponding neutron parameters are freely searched. While the resulting fit is good, it begins to depart from the trend of the data at 25° and beyond. By including a Gaussian correction with $r_0 \approx R_p/2$ in *both* proton and neutron densities we can get the improved fit shown by the solid curve in Fig. 1. This is a rather crude correction¹ and somewhat affects the fit at angles forward of 25° also. While we do not claim that the present matter distributions are in any way unique, we believe the backward-angle data clearly show enough sensitivity to the interior details of the matter distributions to make a further, systematic study along these lines worthwhile. The neutron density parameters for both the dashed and solid curves are given in Table I. For both sets of parameters, $\Delta r_{np} \approx 0.3$ fm.

In summary, data from the first experiment using the HRS facility at LAMPF are presented. These 0.8-GeV proton elastic scattering data ex-

tend over a larger angular range (2° – 40° , for the case of carbon) than have heretofore been investigated near 1 GeV. The data and the accompanying analysis indicate that proton-nucleus scattering at 0.8 GeV may be sensitive to more than just the gross size of the nuclear matter distributions. It encourages the view that comprehensive data and careful, exhaustive analysis can provide solid information concerning details of the nuclear matter distributions, including density fluctuations in the nuclear interior.

This research was supported in part by the U. S. Department of Energy, the Robert A. Welch Foundation, and the National Science Foundation.

¹J. Heisenberg *et al.*, Phys. Rev. Lett. **23**, 1402 (1969).

²I. Sick and J. S. McCarthy, Nucl. Phys. **A150**, 631 (1970).

³C. W. DeJager *et al.*, At. Data Nucl. Data **14**, 479 (1974).

⁴I. Ahmad, Nucl. Phys. **A247**, 418 (1975).

⁵G. D. Alkhozov *et al.*, Nucl. Phys. **A274**, 443 (1976), and Phys. Lett. **67B**, 402 (1977).

⁶L. Ray and W. R. Coker, to be published.

⁷E. Boridy and H. Feshbach, to be published.

⁸H. B. Willard *et al.*, Phys. Rev. C **14**, 1545 (1976).

⁹W. R. Coker *et al.*, Phys. Lett. **64B**, 403 (1976).

¹⁰H. Feshbach *et al.*, Ann. Phys. (N.Y.) **66**, 20 (1971).

¹¹E. Kujawski, Phys. Rev. C **1**, 1651 (1970); E. Kujawski and J. P. Vary, Phys. Rev. C **12**, 1271 (1975).

¹²J. Bystricki *et al.*, Centre d'Etudes Nucléaires de Saclay Report No. CEA-N1547 (E), 1972 (unpublished). O. Benary *et al.*, Lawrence Berkeley Laboratory Report No. UCRL-20000NN (unpublished).

¹³G. W. Hoffmann *et al.*, Bull. Am. Phys. Soc. **22**, 1017 (1977).